

# Universal scaling of plasmonic refractive index sensors

Yen-Kai Chang,<sup>1</sup> Zong-Xing Lou,<sup>1,2</sup> Kao-Der Chang,<sup>3</sup> and Chih-Wei Chang<sup>1,\*</sup>

<sup>1</sup>Center for Condensed Matter Sciences, National Taiwan University, Taipei 10617, Taiwan

<sup>2</sup>Department of Physics, National Taiwan University, Taipei 10617, Taiwan

<sup>3</sup>Nanotechnology Research Center, Industrial Technology Research Institute, Hsinchu 31040, Taiwan

\*cwchang137@ntu.edu.tw

**Abstract:** We establish experimental and numerical evidence that the refractive index sensitivities of various subwavelength plasmonic sensors obey a simple universal scaling relation that the sensitivities linearly increase with  $\lambda_m/n_{eff}$  (where  $\lambda_m$  is the resonant wavelengths and  $n_{eff}$  is the effective refractive index of the environment) and exhibit a slope equal to 1 instead of 2 predicted theoretically. The universal scaling relation is independent of the geometrical structures or contributions of multipolar resonances of individual metal structures (i.e. plasmonic atoms). It is also independent of spatial distributions or field-enhancements of electromagnetic hot spots in coupled metal structures (i.e. plasmonic molecules). The universal scaling relation reveals the fundamental standing wave resonances for all plasmonic atoms and the predominant near-field electric couplings for most plasmonic molecules. The established universal relation also helps to exclude some magnetically coupled plasmonic molecules for practical applications due to their reduced sensitivities.

©2013 Optical Society of America

**OCIS codes:** (250.5403) Plasmonics; (310.6628) Subwavelength structures, nanostructures.

---

## References and links

1. K. M. Mayer and J. H. Hafner, "Localized Surface Plasmon Resonance Sensors," *Chem. Rev.* **111**(6), 3828–3857 (2011).
2. E. Petryayeva and U. J. Krull, "Localized surface plasmon resonance: Nanostructures, bioassays and biosensing-A review," *Anal. Chim. Acta* **706**(1), 8–24 (2011).
3. C. L. Nehl, H. W. Liao, and J. H. Hafner, "Optical properties of star-shaped gold nanoparticles," *Nano Lett.* **6**(4), 683–688 (2006).
4. Y. G. Sun and Y. N. Xia, "Increased sensitivity of surface plasmon resonance of gold nanoshells compared to that of gold solid colloids in response to environmental changes," *Anal. Chem.* **74**(20), 5297–5305 (2002).
5. H. J. Chen, X. S. Kou, Z. Yang, W. H. Ni, and J. F. Wang, "Shape- and size-dependent refractive index sensitivity of gold nanoparticles," *Langmuir* **24**(10), 5233–5237 (2008).
6. L. J. Sherry, S. H. Chang, G. C. Schatz, R. P. Van Duyne, B. J. Wiley, and Y. N. Xia, "Localized surface plasmon resonance spectroscopy of single silver nanocubes," *Nano Lett.* **5**(10), 2034–2038 (2005).
7. L. J. Sherry, R. C. Jin, C. A. Mirkin, G. C. Schatz, and R. P. Van Duyne, "Localized surface plasmon resonance spectroscopy of single silver triangular nanoprisms," *Nano Lett.* **6**(9), 2060–2065 (2006).
8. C. Y. Tsai, S. P. Lu, J. W. Lin, and P. T. Lee, "High sensitivity plasmonic index sensor using slablike gold nanoring arrays," *Appl. Phys. Lett.* **98**(15), 153108 (2011).
9. M. M. Miller and A. A. Lazarides, "Sensitivity of metal nanoparticle surface plasmon resonance to the dielectric environment," *J. Phys. Chem. B* **109**(46), 21556–21565 (2005).
10. Y. C. Chao, H. C. Tseng, K. D. Chang, and C. W. Chang, "Three types of couplings between asymmetric plasmonic dimers," *Opt. Express* **20**(3), 2887–2894 (2012).
11. H. C. Tseng and C. W. Chang, "High displacement sensitivity in asymmetric plasmonic nanostructures," *Opt. Express* **18**(17), 18360–18367 (2010).
12. A. Kinkhabwala, Z. F. Yu, S. H. Fan, Y. Avlasevich, K. Mullen, and W. E. Moerner, "Large single-molecule fluorescence enhancements produced by a bowtie nanoantenna," *Nat. Photonics* **3**(11), 654–657 (2009).
13. E. C. Le Ru and P. G. Etchegoin, "Phenomenological local field enhancement factor distributions around electromagnetic hot spots," *J. Chem. Phys.* **130**(18), 181101 (2009).
14. I. M. Pryce, K. Aydin, Y. A. Kelaita, R. M. Briggs, and H. A. Atwater, "Highly Strained Compliant Optical Metamaterials with Large Frequency Tunability," *Nano Lett.* **10**(10), 4222–4227 (2010).
15. I. M. Pryce, Y. A. Kelaita, K. Aydin, and H. A. Atwater, "Compliant Metamaterials for Resonantly Enhanced Infrared Absorption Spectroscopy and Refractive Index Sensing," *ACS Nano* **5**(10), 8167–8174 (2011).

16. N. Verellen, P. Van Dorpe, C. J. Huang, K. Lodewijks, G. A. E. Vandenbosch, L. Lagae, and V. V. Moshchalkov, "Plasmon Line Shaping Using Nanocrosses for High Sensitivity Localized Surface Plasmon Resonance Sensing," *Nano Lett.* **11**(2), 391–397 (2011).
17. C. Y. Chen, S. C. Wu, and T. J. Yen, "Experimental verification of standing-wave plasmonic resonances in splitting resonators," *Appl. Phys. Lett.* **93**(3), 034110 (2008).
18. F. Neubrech, T. Kolb, R. Lovrincic, G. Fahsold, A. Pucci, J. Aizpurua, T. W. Cornelius, M. E. Toimil-Molares, R. Neumann, and S. Karim, "Resonances of individual metal nanowires in the infrared," *Appl. Phys. Lett.* **89**(25), 253104 (2006).
19. C. Rockstuhl, T. Zentgraf, H. Guo, N. Liu, C. Etrich, I. Loa, K. Syassen, J. Kuhl, F. Lederer, and H. Giessen, "Resonances of split-ring resonator metamaterials in the near infrared," *Appl. Phys. B* **84**(1–2), 219–227 (2006).
20. M. Piliarik, P. Kvasnička, N. Galler, J. R. Krenn, and J. Homola, "Local refractive index sensitivity of plasmonic nanoparticles," *Opt. Express* **19**(10), 9213–9220 (2011).
21. N. Liu, T. Weiss, M. Mesch, L. Langguth, U. Eigenthaler, M. Hirscher, C. Sönnichsen, and H. Giessen, "Planar Metamaterial Analogue of Electromagnetically Induced Transparency for Plasmonic Sensing," *Nano Lett.* **10**(4), 1103–1107 (2010).

## 1. Introduction

Subwavelength metal structures exhibiting plasmonic resonances have enabled widespread interests in their potential applications in chemical sensing and super-resolution imaging. Since the optical responses of these metal structures are largely determined by their geometries, each metal structure can be considered as an artificial atom (plasmonic atom) for light. The great design flexibilities of these plasmonic atoms have led to many extraordinary optical phenomena that can be manipulated by advanced chemical syntheses or nanolithography methods. Because the resonant frequencies of these plasmonic atoms are highly sensitive to the environmental media, they have been utilized as subwavelength refractive index sensors [1, 2]. Previous intensive experimental studies on plasmonic atoms of varieties of geometries, including nanostar [3], nanoshell [4], nanosphere [5], nanocube [6], nanorod [5], nanorice [5], nanoprism [7], and nanoring [8] etc. have stimulated a lot of interests. However, these works mainly focus on the specialties of each plasmonic atoms, very few works have devoted to understanding the universal behavior. Miller and Lazarides have pointed out that the refractive index sensitivities (expressed as resonant wavelength shifts per refractive index unit (RIU)) of various plasmonic atoms should linearly increase with  $\lambda_m/n_{eff}$  (where  $\lambda_m$  is the resonant wavelengths and  $n_{eff}$  is the effective refractive index of the surrounding media) [9]. They also predicted that, due to the dispersion of permittivity of gold at the visible range, the universal scaling relation should exhibit a slope equal to 2 [9]. However, the prediction disagrees with most experimental results that we summarized in Fig. 1, in which the universal scaling appears to fall on a line with a smaller slope for  $\lambda_m/n_{eff}$  in the visible and infrared ranges. Moreover, while the refractive index sensitivities of many plasmonic atoms display an approximately linear relation with respect to  $\lambda_m/n_{eff}$ , some results from nanostars (sensitivity = 594nm/RIU at  $\lambda_m/n_{eff} = 541\text{nm}$ ) show anomalous deviations to the general trend [3]. Although it is argued that the deviations are due to strong multipolar resonances in nanostars whereas they are absent in other structures, it is still not clear about the electromagnetic origin.

Plasmonic sensors are not limited to plasmonic atoms. Coupling two or more plasmonic atoms into plasmonic molecules can lead to rich phenomena, including nontrivial frequency shifts [10], redistributions of electromagnetic hot spots and the field-enhancements [11]. Although it has been known that the presence of the electromagnetic hot spots are necessary for enhancing Raman scatterings and fluorescence [12, 13], their roles in sensing the environmental refractive index remain unclear. Unfortunately, comparing to the intensive studies on plasmonic atoms, much fewer works were done in plasmonic molecules [14–16]. Besides, it is not clear whether the refractive index sensitivities of plasmonic molecules would obey a universal relation similar to plasmonic atoms.

Because elucidating the universal phenomena of the plasmonic sensors with diverse geometries and couplings will be of fundamental importance for practical applications, here we provide key experimental and numerical evidence that the linear scaling relation is a universal property of surface plasmons. In fact, the universal scaling relation established in

Fig. 1 is a direct result of the standing wave resonances of surface plasmons and is insensitive to geometrical variations of plasmonic atoms or couplings in most plasmonic molecules. Our experimental results show that it is also independent of the nature of dipolar or multipolar resonances, the distributions or field-enhancements of the electromagnetic hot spots. The established universal behavior also helps to exclude some unlikely theoretical or experimental results reported earlier.

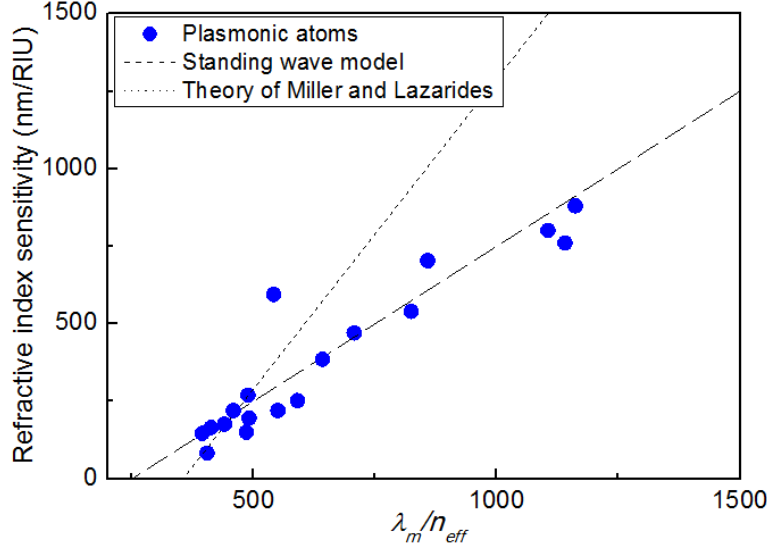


Fig. 1. Summarized refractive index sensitivities vs.  $\lambda_m/n_{eff}$  of various plasmonic atoms reported in earlier experiments (Ref [1–8]). The theoretical predictions by Miller and Lazarides (Ref [9], dotted line) and the standing wave model (Eq. (2), dashed line) are shown for comparison.

We start the investigation on the simplest plasmonic atoms with geometries like a rod or a split-ring resonator (SRR). The resonant frequencies of a metal rod or a SRR can be characterized by the one-dimensional standing wave model of surface plasmons [17]:

$$\lambda_m = 2n_{eff} \left( \frac{L}{m} \right) - \lambda_0 \quad (1)$$

where  $\lambda_m$  is the resonant wavelength of the  $m$ -th harmonic mode,  $L$  is the total length of the rod or the SRR,  $n_{eff}$  is the effective refractive index of the environment, and  $\lambda_0$  is a geometrically dependent offset. The standing wave model has been experimentally and numerically verified in rods and SRRs at the fundamental mode ( $m = 1$ ) and at higher harmonic resonances ( $m > 1$ ) as well [17–19]. Note that for  $m = 1$ , the resonances are dominated by electric/magnetic dipoles, whereas they contain significant contributions from multipolar modes when  $m > 1$ . From Eq. (1), we can easily obtain the refractive index sensitivities ( $d\lambda_m/dn_{eff}$ ) of rods or SRRs:

$$\frac{d\lambda_m}{dn_{eff}} = \frac{\lambda_0}{n_{eff}} + \left( \frac{\lambda_0}{n_{eff}} - \frac{d\lambda_0}{dn_{eff}} \right) \quad (2)$$

Equation (2) shows that the refractive index sensitivities increase with  $\lambda_m/n_{eff}$  with a slope equal to 1 and an offset  $-250\text{nm/RIU}$  (obtained from the fit in Fig. 1). Importantly, the refractive index sensitivity is independent of the harmonic number  $m$ . Thus the presence of multipolar resonances does not affect the universal scaling relation. Finally, generalizing the

result to two or three dimensions with complex structures will introduce a small geometrical correction factor to  $\lambda_0$  and will yield similar results like Eq. (2). We thus plot the prediction of Eq. (2) as the dashed line in Fig. 1. Note that  $n_{eff} = 1.33$  for plasmonic atoms suspended in water. For those dispersed in glass slides, we have employed simulations to determine the  $n_{eff}$  (see supporting information). Clearly, the experimental data of most plasmonic atoms fall on the dashed line, suggesting that the standing wave model is applicable to diverse geometries and the geometrical corrections to the complex structures remain small. In addition, we have found that the anomalous deviations to the universal scaling relation in nanostars can be attributed to the inconsistencies of the experimental data [3]. Therefore, we conclude that the standing wave model explains the refractive index sensitivities of all plasmonic atoms known so far.

## 2. Methods

It will be interesting to see whether plasmonic molecules would follow identical universal scaling relation shown in Fig. 1. Naively, one may speculate that due to the strong near-field couplings, the enhanced multipolar contributions, the field-enhancements, and re-distributions of electromagnetic hot spots, deviations to the universal scaling relation may occur in plasmonic molecules. To investigate their effects on the refractive index sensitivities and the universal relation, we have designed and fabricated three kinds of plasmonic molecules with asymmetric structures (Fig. 2(a, b) and Fig. 3(a, b)). Coupling two plasmonic atoms into a plasmonic molecule always leads to complex interactions between different resonant modes. Recently we have categorized the complex interactions into three types of couplings [10]. Among them, the Type III coupling that contains two redshifts in resonant wavelengths is particularly interesting because they do not have any mechanical analogies. The fabricated Molecules A, B, and C all belong to the Type III coupling. Moreover, the distances between of constituted elements can be artificially designed so that the coupling strength, the resonant frequencies, the multipolar contributions, the hot spot distributions, and the field-enhancements can be controlled via advanced electron beam lithography (Elionix ELS 7000). Experimentally, we fabricated arrays ( $40\mu\text{m} \times 40\mu\text{m}$ ) of plasmonic molecules by patterning 40nm thick Au films on quartz substrates. The inter-molecular separations ( $s$ ) were varied from 11nm to 20nm and their refractive index sensitivities were characterized by measuring the transmitted spectra using an infrared spectrometer equipped with a broadband light source. We also employed finite difference time domain simulation using commercial software CST Microwave Studio to assist our analyses. The electrical conductivity of gold is described by the Drude model with plasmon frequency  $2.175 \times 10^{15}$  Hz and a practical damping rate  $1.2 \times 10^{14}$  Hz.

## 3. Results and discussions

Figures 2(c-f) show the simulated electric field and surface current distributions of the fabricated plasmonic molecules (Molecules A and B) with  $s = 20\text{nm}$ . The asymmetric structures of Molecules A and B allow both antisymmetric and symmetric resonant modes to be observed at the far field. Particularly, both the antisymmetric resonant modes of Molecules A and B exhibit antiparallel surface currents and thereby contain large contributions from electric quadrupoles. On the other hand, the symmetric modes are dominated by electric and magnetic dipolar resonances. Moreover, the hot spots appearing at the edges of the structures exhibit field-enhancements more than 25-fold and they are also dependent on the resonant modes. As shown in Figs. 2(c-f), the hot spots are much larger in the antisymmetric modes than those in the symmetric modes. Thus the design of Molecules A and B allows experimental investigations on the effects of different electric quadrupolar contributions as well as the hot spot distributions to the refractive index sensitivities.

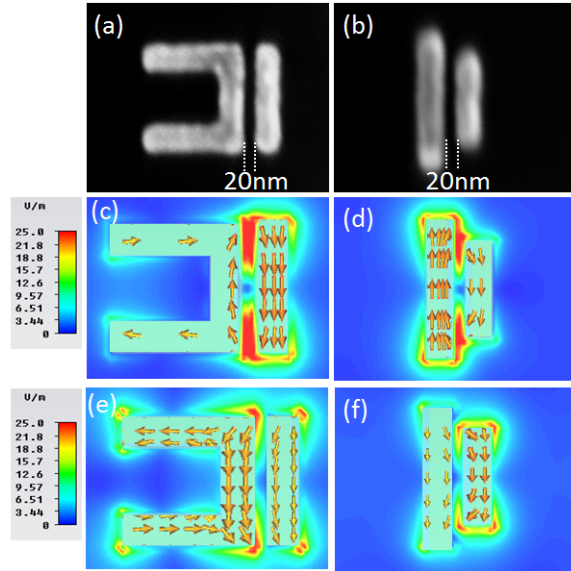


Fig. 2. (a, b) SEM images of the fabricated Molecules A and B with inter-molecular separation  $s = 20\text{nm}$ . (c, d) Electric field (hot spot) distributions of Molecules A and B at the respective antisymmetric resonant modes. (e, f) Electric field (hot spot) distributions of Molecules A and B at the respective symmetric resonant modes. The arrows denote the flows of the surface currents.

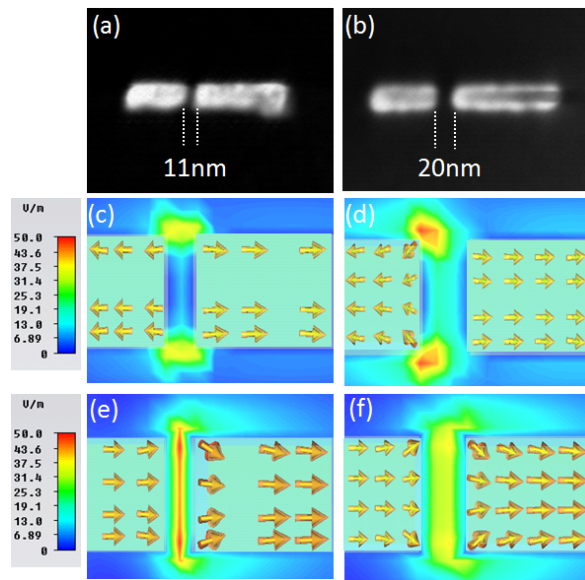


Fig. 3. (a, b) SEM images of the fabricated Molecules C with inter-molecular separation  $s = 11\text{nm}$  and  $20\text{nm}$ . (c, d) Electric field (hot spot) distributions at the respective antisymmetric resonant modes. (e, f) Electric field (hot spot) distributions at the respective symmetric resonant modes. The arrows denote the flows of the surface currents. Note that the field-enhancement is more pronounced for the symmetric mode at  $s = 11\text{nm}$ .

Because the associated field-enhancements at the hot spots not only depend on the resonant modes but also strongly correlate with the inter-molecular interactions, we have also fabricated Molecule C with  $s$  varied from  $20\text{nm}$  to  $11\text{nm}$ . As shown in Figs. 3(a, b), the sharp edges persist during the experimental lift-off processes even though  $s$  is reduced to  $11\text{nm}$ . For

the symmetric mode, the field-enhancements shown in Figs. 3(e, f) are at least 30-fold for  $s = 20\text{nm}$  and can be more than 50-fold when  $s$  is reduced to 11nm. Thus the genuine effect of field-enhancements on the refractive index sensitivities can be investigated in the two Molecule C's.

Figures 4(a-d) show measured transmission spectra of Molecules A, B, and C ( $s = 20\text{nm}$  and 11nm). The refractive index sensitivities are tested using water ( $n = 1.33$ ). The resonant wavelength redshifts ( $\Delta\lambda_m$ ) is 191nm (antisymmetric mode) for Molecule A,  $\Delta\lambda_m = 160\text{nm}$  (symmetric mode) and 175nm (antisymmetric mode) for Molecule B. For the symmetric mode of Molecule C, we obtain  $\Delta\lambda_m = 178\text{nm}$  for  $s = 20\text{nm}$  and  $\Delta\lambda_m = 206\text{nm}$  for  $s = 11\text{nm}$ . The measured spectra are consistent with the simulation results.

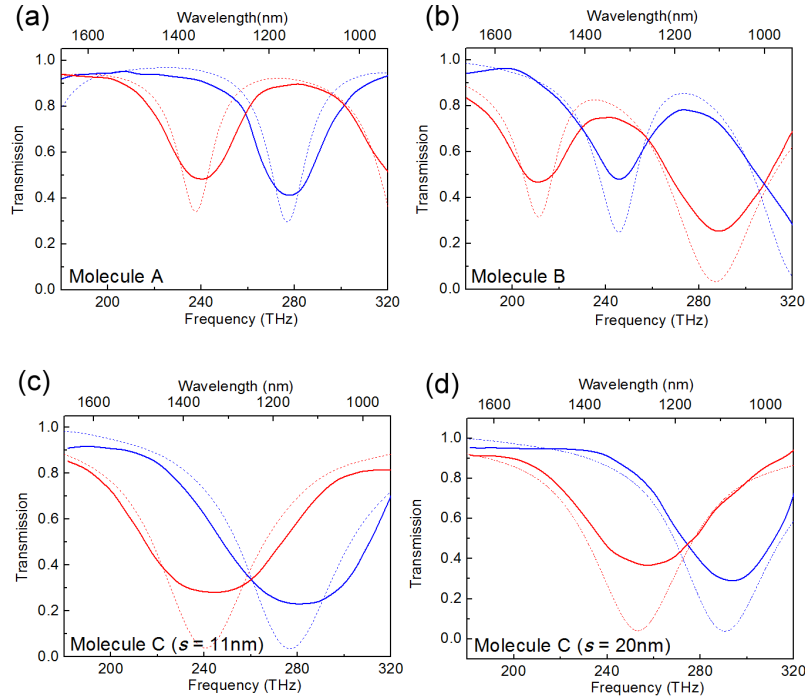


Fig. 4. Experimental (solid curves) and simulated (dashed curves) transmission spectra of Molecules (a) A, (b) B, (c) C ( $s = 11\text{nm}$ ), and (d) C ( $s = 20\text{nm}$ ) before (blue curves) and after (red curves) dropping water refractive index tests.

We note that while most previous experiments on plasmonic atoms were tested in water ( $n = 1.33$ ), the plasmonic molecules were generally fabricated on a solid substrate like quartz or sapphire. To compare the results with those of plasmonic atoms, the contributions from the substrates should be included (see supporting information). In our work, Molecules A, B, and C are fabricated on a quartz substrate ( $n = 1.53$ ). When they are measured in air, the situation can be equivalent to these Molecules being immersed into a media with homogeneous effective refractive index ( $n_{eff}$ ). By employing numerical simulations, we determine  $n_{eff} = 1.18$  for quartz substrates. Similarly, when they are measured in water, they are equivalent to being immersed into a media with  $n_{eff} = 1.43$ . After incorporating the corrections on  $n_{eff}$ , we can experimentally determine  $d\lambda_m/dn_{eff}$  and  $\lambda_m/n_{eff}$ . The data are plotted in Fig. 5(a).

Clearly, the refractive sensitivities of Molecules A, B, and C still follow the same universal scaling relation established for plasmonic atoms. In addition, although reducing the  $s$  makes the structure more asymmetric and thereby enhances the multipolar contributions, the refractive index sensitivities do not deviate away from the universal scaling. Furthermore, the field enhancements or the redistribution of the hot spots do not affect the universal scaling relation, either. In fact, hot spot distributions are known to affect the sensitivities to local

refractive index variations [20], whereas they remain unaffected for bulk refractive index measurements. We have applied similar methods to plasmonic molecules studied by previous works (see supporting information) [14–16]. As shown in Fig. 5(a), the universal scaling relation applies to different geometries of plasmonic molecules studied so far.

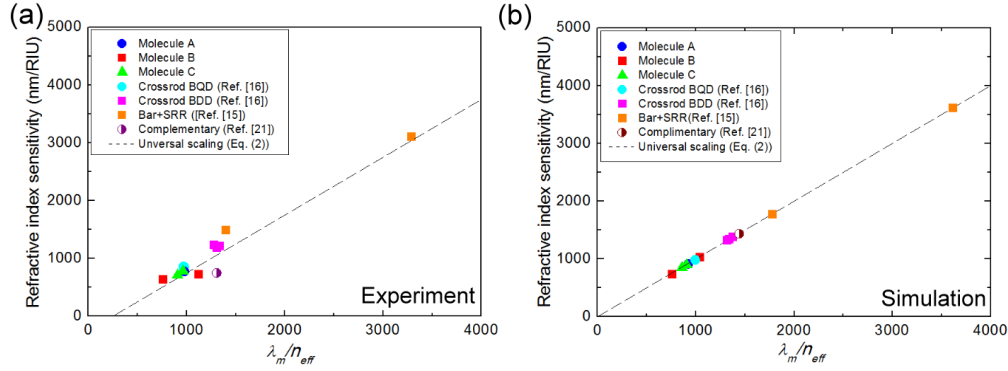


Fig. 5. Summarized (a) experimental and (b) simulated (without substrates) refractive index sensitivities vs.  $\lambda_m/n_{eff}$  of various plasmonic molecules. The universal scaling relation established in Eq. (2) is shown as the dashed line.

To understand the universal scaling relation established for plasmonic molecules, we note that from dimensional analyses, coupling two or more plasmonic atoms into plasmonic molecules will result in new resonant frequencies expressed by the general formulation:

$$\omega = \omega_a + \frac{M_e}{\sqrt{\epsilon}} + \sqrt{\mu M_m} \quad (3)$$

where  $\omega_a$  is the resonant frequency of the uncoupled plasmonic atom,  $M_e$  is a function independent of  $\epsilon$ , and  $M_m$  is a function independent of  $\epsilon$  and  $\mu$ . The last two terms of Eq. (3) together represent the couplings. Experimentally, because no magnetic responses can be observed at optical frequencies,  $\mu = 1$  and  $dM_e/dn_{eff} = dM_m/dn_{eff} = 0$ . The slope of  $d\lambda_m/dn_{eff}$  vs.  $\lambda_m/n_{eff}$  of plasmonic molecules thus follows:

$$\frac{d\lambda_m/dn_{eff}}{\lambda_m/n_{eff}} = -\frac{d\omega/dn_{eff}}{\omega/n_{eff}} = \frac{-d\omega_a/dn_{eff} + M_e/n_{eff}^2}{\omega_a/n_{eff} + M_e/n_{eff}^2 + M_m/n_{eff}} \quad (4)$$

Because plasmonic atoms follow  $(d\omega_a/dn_{eff})/(\omega_a/n_{eff}) = -1$  and the coupling strengths ( $M_e$ ,  $M_m$ ) are always smaller than the  $\omega_a$ , Eq. (4) can be approximated to

$$\frac{d\lambda_m/dn_{eff}}{\lambda_m/n_{eff}} \approx 1 - O\left(\frac{M_m}{\omega_a}\right) \quad (5)$$

The last term denotes corrections to the order of  $M_m/\omega_a$ . Thus we learn that the slope will be close to 1 if the interactions of the plasmonic molecules are not dominated by magnetic interactions. The result is numerically confirmed in Fig. 5(b), in which the effects from the substrates are removed (i.e.  $n_{eff} = 1$ ) by simulation. From Fig. 5(b), we learn that most plasmonic molecules studied so far follow the universal scaling relation, suggesting the predominant electric couplings. Experimentally, so far notable deviations to the universal scaling are found in complementary plasmonic molecules only [21]. However, the anomalous deviation is not confirmed by simulations. From an application's point of view, we also learn that plasmonic molecules with strong magnetic interactions will not be suitable for practical applications due to their reduced refractive index sensitivities.

In summary, we established a universal scaling relation for refractive sensitivities of various plasmonic atoms and molecules operating in the visible or infrared ranges. In general, the refractive index sensitivities increase with respect to  $\lambda_m/n_{eff}$  and exhibit a slope equal to 1. The universal scaling is independent of the structures of the subwavelength metals, multipolar contributions, field-enhancements, hot spot distributions, or couplings in most cases. We find the universal scaling relation can be explained by the standing wave model of surface plasmons for all plasmonic atoms and the predominant electric couplings for most plasmonic molecules studied so far.

### **Acknowledgments**

We thank Dr. Wei-Li Lee's supports on nanofabrication. This work was supported by the National Science Council of Taiwan (NSC101-2112-M-002-014-MY3).

# Universal scaling of plasmonic refractive index sensors: erratum

Yen-Kai Chang,<sup>1,2</sup> Zong-Xing Lou,<sup>1,2</sup> Kao-Der Chang,<sup>3</sup> and Chih-Wei Chang<sup>1,\*</sup>

<sup>1</sup>Center for Condensed Matter Sciences, National Taiwan University, Taipei 10617, Taiwan

<sup>2</sup>Department of Physics, National Taiwan University, Taipei 10608, Taiwan

<sup>3</sup>Nanotechnology Research Center, Industrial Technology Research Institute, Hsinchu 31040, Taiwan

\*[cwchang137@ntu.edu.tw](mailto:cwchang137@ntu.edu.tw)

**Abstract:** Corrections to the author affiliations and Eq. (3) in the paper [Opt. Express 21(2), 1804-1811 (2013)].

©2013 Optical Society of America

**OCIS codes:** (250.5403) Plasmonics; (310.6628) Subwavelength structures, nanostructures.

---

## References and links

1. Y. K. Chang, Z. X. Lou, K. D. Chang, and C. W. Chang, "Universal scaling of plasmonic refractive index sensors," Opt. Express **21**(2), 1804–1811 (2013).

- 
1. The first author's affiliations of Ref. [1] should be corrected to: Yen-Kai Chang,<sup>1,2</sup> Zong-Xing Lou,<sup>1,2</sup> Kao-Der Chang,<sup>3</sup> and Chih-Wei Chang<sup>1,\*</sup>

<sup>1</sup>Center for Condensed Matter Sciences, National Taiwan University, Taipei 10617, Taiwan

<sup>2</sup>Department of Physics, National Taiwan University, Taipei 10608, Taiwan

<sup>3</sup>Nanotechnology Research Center, Industrial Technology Research Institute, Hsinchu 31040 Taiwan

2. Equation (3) in the Ref [1]. should be corrected to:

$$\omega = \omega_a + \frac{M_c}{\sqrt{\epsilon}} + \sqrt{\mu} M_m \quad (3)$$